

# Circumnavigating Misfolding Traps in the Energy Landscape through Protein Engineering: Suppression of Molten Globule and Aggregation in Carbonic Anhydrase<sup>†</sup>

Martin Karlsson, Lars-Göran Mårtensson,\* Patrik Olofsson, and Uno Carlsson\*

*IFM-Department of Chemistry, Linköping University, SE-581 83 Linköping, Sweden*

*Received February 9, 2004; Revised Manuscript Received March 18, 2004*

**ABSTRACT:** The native state of the enzyme human carbonic anhydrase (HCA II) has been stabilized by the introduction of a disulfide bond, the oxidized A23C/L203C mutant. This stabilized protein variant undergoes an apparent two-state unfolding process with suppression of the otherwise stable equilibrium, molten-globule intermediate, which is normally very prone to aggregation. Stopped-flow measurements also showed that lower amounts of the transiently occurring molten globule were formed during refolding. This led to a markedly lowered tendency for aggregation during equilibrium denaturing conditions and, more importantly, to significantly higher reactivation yields upon refolding of the fully denatured protein. Thus, a general strategy to circumvent aggregation during the refolding of proteins could be to stabilize the native state of a protein at the expense of partially folded intermediates, thereby shifting the unfolding behavior from a three-state process to a two-state one.

Protein aggregation is a major concern for biotechnology and biomedicine, as well as for *in vitro* studies aimed at investigating the mechanism of protein folding. In addition, protein aggregation has recently been shown to cause numerous diseases, such as Alzheimer's disease, Parkinson's disease, and prion diseases.

In our ongoing folding studies, we use human carbonic anhydrase II (HCA II)<sup>1</sup> as a model protein (1, 2). It has a molecular mass of 29.3 kDa and is essentially a  $\beta$ -sheet protein, containing a large hydrophobic core (3, 4). Unfolding of the protein has been demonstrated to be a three-state process with the formation of a stable, molten-globule intermediate at moderate denaturing pressure (5, 6). This molten-globule, equilibrium intermediate, including some of its most apolar  $\beta$  strands (7), is prone to aggregation and has been shown to form aggregates in a very specific manner. Aggregation during refolding also leads to incomplete recovery of the native protein, which can be prevented by the action of the chaperonin GroEL (8).

Recently, we succeeded in dramatically stabilizing the native state of HCA II by engineering a disulfide bond into the protein structure (the oxidized A23C/L203C mutant; Figure 1). This stabilized protein variant undergoes an apparent two-state unfolding process with suppression of the

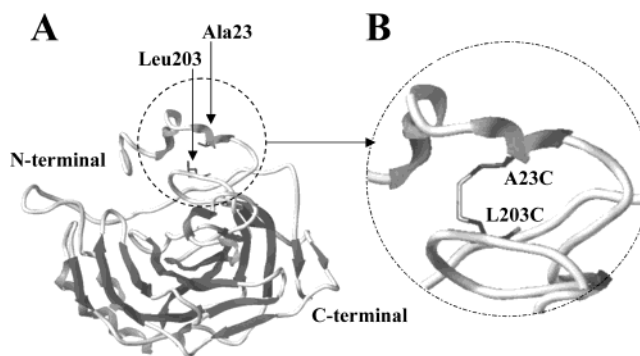


**FIGURE 1:** (A) Overall structure of HCA II [PDB 2CBA (4)] with the side chains of Ala 23 and Leu 203 marked and encircled. (B) Enlargement of the encircled area showing a model of the oxidized form of the double mutant A23C/L203C. This figure is modified from Figure 1 in ref 9.

otherwise stable equilibrium, molten-globule intermediate (9). Therefore, in this paper, we investigated whether stabilization of the native conformation, at the expense of the molten-globule state, can be a strategy to avoid the formation of aggregates at equilibrium conditions. The primary objective was to see if stabilization of the native state and thus suppression of the equilibrium, molten globule also leads to suppression of the transient molten globule that is an intermediate in the refolding process of HCA II (10). The appearance of a kinetic molten-globule intermediate causes a fraction of the molecules to become trapped in aggregates and leads to reduced refolding yields of the active enzyme (11–13). Our data clearly show that this strategy of stabilizing the enzyme works in the case of carbonic anhydrase and this approach could be a general way to circumvent the formation of aggregates during the folding process.

<sup>†</sup> This work was supported by the Swedish Research Council (U.C. and L.-G.M.) and Stiftelsen Lars Hiertas Minne (M.K.).

\* To whom correspondence should be addressed. E-mail: ucn@ifm.liu.se. Phone: +46-13-281714. Fax: +46-13-281399 (U.C.); E-mail: lgmar@ifm.liu.se (L.-G.M.).

<sup>1</sup> Abbreviations: A23C/L203C<sub>red</sub>, reduced form of HCA II<sub>pwt</sub> with the mutations Ala23 → Cys and Leu203 → Cys; A23C/L203C<sub>ox</sub>, oxidized form of HCA II<sub>pwt</sub> with the mutations Ala23 → Cys and Leu203 → Cys; ANS, 8-anilino-1-naphthalenesulfonic acid; BCA II, bovine carbonic anhydrase II; GuHCl, guanidine hydrochloride; HCA II<sub>pwt</sub>, pseudo-wild-type human carbonic anhydrase II, with a Cys206 → Ser mutation.

## MATERIAL AND METHODS

**Chemicals.** Guanidine-HCl (GuHCl) was purchased from Pierce, and the concentration of the solution was determined by the refractive index (14). 8-Anilino-1-naphthalene sulfonic acid (ANS) was obtained from Sigma. All other chemicals were of reagent grade.

**Protein Expression and Purification.** The HCA II mutant with an engineered disulfide bond (A23C/L203C) used in this paper was made using the cysteine-free C206S pseudo-wild-type protein (HCA II<sub>pwt</sub>) as a template, as described earlier (9). Bovine carbonic anhydrase II (BCA II) was prepared from cattle erythrocytes. The initial preparation and chromatographic purification of BCA II were carried out according to Lindskog (15) and subsequently followed by affinity chromatography (16).

**Unfolding Measurements.** The unfolding profile of the HCA II variants was determined by intrinsic Trp fluorescence measurements as previously described (9).

**Refolding Yield Measurements.** The HCA II variants (14.2  $\mu$ M) were denatured for 24 h in various concentrations of GuHCl (0.5–5 M) buffered with 0.1 M Tris-H<sub>2</sub>SO<sub>4</sub> at pH 7.5. The denaturing solution containing the reduced A23C/L203C mutant was also supplemented with a 1000-fold molar excess of reduced DTT (dithiothreitol). Refolding was initiated by dilution of the denatured enzyme solution to 0.3 M GuHCl and a final protein concentration of 0.85  $\mu$ M (0.025 mg/mL). The CO<sub>2</sub>-hydration activity of the enzyme was measured after 2 h of refolding. The enzyme activity assay has previously been described (17).

**Refolding Kinetic Measurements.** The reactivation kinetics were measured at 23 °C after denaturation of the HCA II variants (14.2  $\mu$ M) in 5 M GuHCl for 1 h. Reactivation was achieved by rapidly diluting to 0.3 M GuHCl and a protein concentration of 0.85  $\mu$ M. All solutions were buffered with 0.1 M Tris-H<sub>2</sub>SO<sub>4</sub> at pH 7.5. The refolding reaction was monitored by measuring the recovery of the CO<sub>2</sub>-hydration activity (17). Using a nonlinear least-squares program (TableCurve, Jandel Scientific), kinetic reactivation data were fit with a series of exponential terms.

**Sequential Mixing Stopped Flow.** All kinetic experiments were performed at 23 °C on an SX.18MV-R stopped-flow reaction analyzer (Applied Photophysics) equipped with a SQ1 sequential flow accessory. Excitation was performed at 360 nm, with a bandwidth of 5 nm, in a 20- $\mu$ L cell. The emission was collected via the fluorometric port of the cell, through an optical filter with a cutoff at 455 nm. Before the measurements, the photomultiplier tube voltage and offset were adjusted using the folded protein (1.7  $\mu$ M) and a 40 times molar excess of ANS in 0.3 M GuHCl to bring the signal to zero with the folded protein mixed with ANS in the cell.

The protein (34  $\mu$ M) was denatured for 1 h by 3 M GuHCl at 23 °C. The first mixing stage (total volume of 300  $\mu$ L) was used to refold the protein to a concentration of 3.4  $\mu$ M in 0.3 M GuHCl, in a 115- $\mu$ L aging loop, by a 1:10 dilution with 0.1 M Tris-H<sub>2</sub>SO<sub>4</sub> at pH 7.5. After various delay times, the refolding protein was mixed in a 1:2 ratio with ANS (136  $\mu$ M) in 0.3 M GuHCl in a second stage, to a final concentration of 1.7  $\mu$ M in 0.3 M GuHCl with a 40 molar excess of ANS. The binding of ANS to the folding protein was monitored for 5 s, and the data reported for the kinetics

of the interaction between the folding protein and ANS originate from the first data point. The shortest possible aging time with the setup used was 35 ms, as reported by the instruments software, whereas the dead time between the protein and ANS mixing and collection of the first data point was about 3 ms. For each delay time, six consecutive runs were made in a short period of time, of which the first two were discarded because these often showed signs of being influenced by the diffusion in the tubing. The small increase of fluorescence intensity upon interaction between ANS and the native protein in 0.3 M GuHCl was also recorded for reference purposes. This reference trace was subtracted from all experimental traces before the value of the first data point was determined. All data were collected with the drive pressure held constant through the 5-s measurement because this gave more reproducible data and did not influence the refolding. All solutions were buffered with 0.1 M Tris-H<sub>2</sub>SO<sub>4</sub> at pH 7.5.

## RESULTS AND DISCUSSION

**Disulfide Bond Variant.** The disulfide bond variant investigated in this paper (A23C/L203C) was engineered from a pseudo-wild-type template (HCA II<sub>pwt</sub>) in which a C206S mutation was made to replace the single cysteine in the wild-type protein. This was made to avoid the unwanted formation of intermolecular disulfide bonds. We have previously shown that HCA II<sub>pwt</sub> has properties that are indistinguishable from those of the wild type (5). The oxidized variant with the disulfide bond intact (A23C/L203C<sub>ox</sub>) and the reduced variant with two free SH-groups (A23C/L203C<sub>red</sub>) were both studied in this paper.

**Unfolding of the HCA II Variants.** The equilibrium unfolding behavior of the HCA II variants is illustrated in Figure 2A, where the dependence of the Trp fluorescence on the concentration of the denaturing agent GuHCl is shown. As can be seen, HCA II<sub>pwt</sub> and A23C/L203C<sub>red</sub> unfold with two separated transitions via a stable folding equilibrium intermediate (N  $\rightarrow$  I  $\rightarrow$  U). This intermediate has been shown to have characteristics that are typical for a molten globule (5, 6, 9). On the other hand, the unfolding of A23C/L203C<sub>ox</sub> shows a two-state pattern. The total red-shift of the Trp fluorescence demonstrates that all of the protein variants totally unfold to the same degree regarding Trp exposure, which also means that the starting states of the variants are similar in the performed refolding experiments described below.

**Aggregation Behavior at Equilibrium.** Previously, we have shown that the molten-globule intermediate of HCA II is prone to aggregation at equilibrium conditions. Thus, if HCA II is denatured at GuHCl concentrations promoting the molten-globule state (1–2 M), the recovery of the active enzyme upon dilution of the denaturant is drastically reduced. This is due to irreversibly formed aggregates by the molten-globule intermediate (7). For A23C/L203C<sub>red</sub>, similar to HCA II<sub>pwt</sub>, the refolding yield was significantly decreased when refolding was performed on the protein that was denatured by lower concentrations of GuHCl (Figure 2B). The reactivation yield is inversely reflected by the two unfolding curves N  $\rightarrow$  I and I  $\rightarrow$  U, respectively, leading to a “refolding trough” (7, 18). This demonstrates that the amount of protein that can be correctly folded decreases in parallel with the increase in I formed (molten globule) at both transitions.

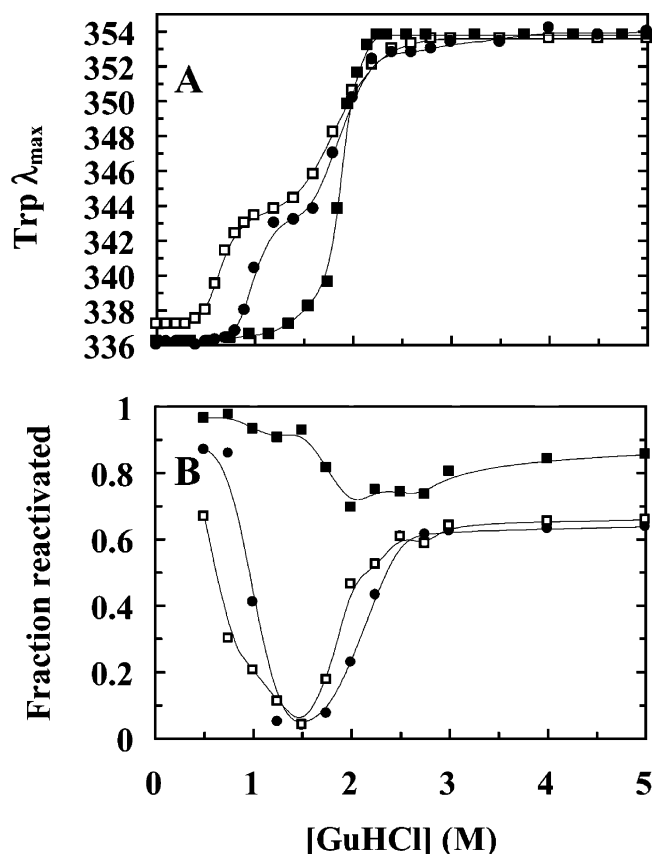


FIGURE 2: (A) Unfolding profiles of the protein variants in the presence of increasing concentrations of denaturant. Symbols: (●) HCA II<sub>pwt</sub>, (■) A23C/L203C<sub>ox</sub>, and (□) A23C/L203C<sub>red</sub>. This figure is modified from the data presented in Figure 3A in ref 9. (B) Refolding yield of the proteins after incubation in various denaturant concentrations. Symbols: (●) HCA II<sub>pwt</sub>, (■) A23C/L203C<sub>ox</sub>, and (□) A23C/L203C<sub>red</sub>.

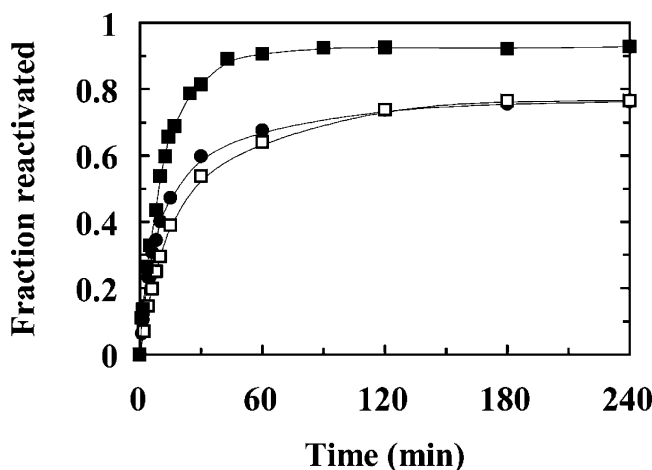


FIGURE 3: Time course of reactivation of completely denatured HCA II variants. The kinetic data were best fitted to two-exponential terms for HCA II<sub>pwt</sub> and A23C/L203C<sub>red</sub> and to one-exponential term for A23C/L203C<sub>ox</sub>. Symbols: (●) HCA II<sub>pwt</sub>, (■) A23C/L203C<sub>ox</sub>, and (□) A23C/L203C<sub>red</sub>.

A23C/L203C<sub>ox</sub> does not seem to form any stable folding intermediate at equilibrium (Figure 2A). The hydrophobic fluorescent dye ANS can be used to probe the existence of the molten-globule intermediate, and earlier reported ANS-binding studies (9; Figure 3B) revealed that a molten-globule intermediate is also formed for A23C/L203C<sub>ox</sub> but to a much lesser extent (5–10% compared to HCA II<sub>pwt</sub> and A23C/

Table 1: Kinetic Parameters of Reactivation

protein	$k_1$ (min <sup>-1</sup> ) <sup>a</sup>	$A_1$ <sup>a</sup>	$k_2$ (min <sup>-1</sup> ) <sup>a</sup>	$A_2$ <sup>a</sup>	$r^2$ <sup>b</sup>
HCA II <sub>pwt</sub>	0.18	0.38	0.02	0.38	0.9993
A23C/L203C <sub>ox</sub>	0.08	0.93			0.9994
A23C/L203C <sub>red</sub>	0.08	0.38	0.02	0.39	0.9936

<sup>a</sup> The rate constants and amplitudes were calculated using a nonlinear fit program (see the Materials and Methods). The amplitudes correspond to fractional reactivation. <sup>b</sup> The goodness of fit was calculated by the  $r^2$  coefficient of determination.

L203C<sub>red</sub>). The decreased formation of the molten globule occurs according to the ANS-binding data with a maximum at 2.0 M GuHCl, i.e., during the global unfolding transition for this variant (9). In Figure 2B, it can be seen that the corresponding drop in the reactivation yield is markedly decreased for A23C/L203C<sub>ox</sub> when it is denatured at GuHCl concentrations between 1 and 2 M that otherwise cause major aggregation problems. The reactivation yield minimum was 70% after denaturation at 2.0 M GuHCl compared to about only 5% for HCA II<sub>pwt</sub> and A23C/L203C<sub>red</sub>. Thus, it is clear that the noted avoidance of aggregation is due to suppression of the equilibrium molten-globule intermediate formed during denaturation.

**Refolding of the Denatured Protein.** Refolding of HCA II that has been globally, completely unfolded only yields about 75% of active HCA II under optimal experimental conditions (7, 19). The reason for the reduced recovery of the native enzyme is that aggregation occurs during the refolding process (11–13). To obtain full reactivation, the assistance of a chaperone such as GroEL is needed, which, by binding to the molten-globule intermediate, prevents it from aggregating (7, 8). The time course of the reactivations of HCA II<sub>pwt</sub>, A23C/L203C<sub>red</sub>, and A23C/L203C<sub>ox</sub> after denaturation for 1 h with 5 M GuHCl is shown in Figure 3. From these data, it is evident that denatured A23C/L203C<sub>ox</sub> can be reactivated to a significantly higher degree (95%) than the other variants (75%). A similar trend was also observed in the “refolding trough” experiments (85 and 65% yield, respectively; Figure 2B). It should be pointed out that the denaturation time in the latter experiments was 24 h; thus, the somewhat lower yields indicate that some irreversible slow aggregation also occurs in the fully unfolded state.

From the time courses of reactivation, it is observed that A23C/L203C<sub>ox</sub> reaches the native state more rapidly than HCA II<sub>pwt</sub> and A23C/L203C<sub>red</sub> (Figure 3). However, a more detailed analysis shows that the reactivation kinetics of A23C/L203C<sub>ox</sub> can be described by a single-exponential expression in contrast to the two-phase kinetics noted for the other variants (Table 1).

This indicates that HCA II<sub>pwt</sub> and A23C/L203C<sub>red</sub> each has one slow and one fast reactivating population, whereas the formation of the disulfide bridge appears to lock more than 90% of the A23C/L203C<sub>ox</sub> molecules in the fast reactivating population. It should be noted that the rate of reactivation for the fast folders is identical for A23C/L203C<sub>ox</sub> and A23C/L203C<sub>red</sub>. Note also that the fast reactivating population (38%) of HCA II<sub>pwt</sub> is about twice as fast as the corresponding population of A23C/L203C<sub>ox</sub>. This means that the important effect of the introduced disulfide bridge is to shift the populations in favor of essentially only fast reactivating molecules. The observed effects on the kinetic parameters can be explained in molecular terms by: (i) The disulfide



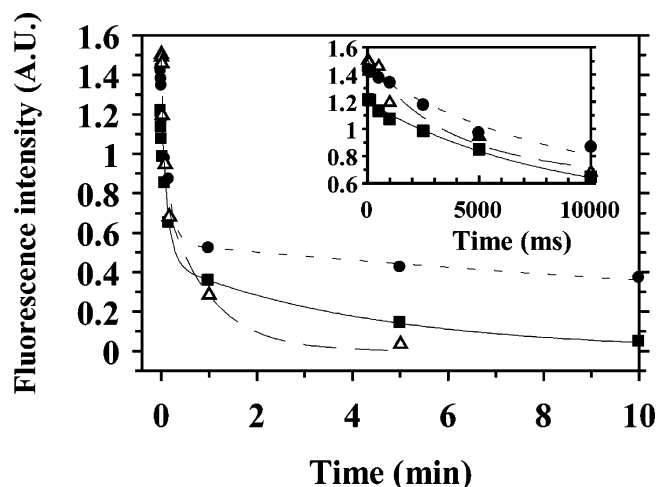


FIGURE 4: Disappearance of the molten-globule intermediate during refolding. This step is monitored by sequential mixing stopped-flow measurements as the change of the ANS fluorescence signal upon binding to the protein after various times of refolding, as indicated by the symbols (for details see the Materials and Methods). Inset: Initial phase is shown. The curves were obtained after fitting to the sum of two-exponential terms. Symbols: ( $\Delta$ , ---) BCA II, ( $\bullet$ , ..... ) HCA II<sub>pw<sub>t</sub></sub>, and ( $\blacksquare$ , —) A23C/L203C<sub>ox</sub>.

bridge causing a reduction of the conformational freedom in the unfolded state. The rate-limiting step during the reactivation of unfolded HCA II has been demonstrated to be the *cis*–*trans* isomerization of peptidyl-prolyl bonds, probably involving the two *cis*-prolines (P30 and P202) present in the HCA II structure (19). Because the introduced disulfide bond between positions 23 and 203 is located close to these *cis*-prolines, it is possible that their native conformations are maintained in the unfolded state to a higher degree than when this linkage is absent. This will lead to a more uniform ensemble of unfolded molecules that will fold to the native conformation from an apparent single state. (ii) Circumventing or suppressing the folding intermediates such as the molten globule that form aggregates or misfolded states (11, 13).

The fact that the yield of reactivated A23C/L203C<sub>ox</sub> from the fully denatured state is significantly higher than can be obtained for HCA II<sub>pw<sub>t</sub></sub> and A23C/L203C<sub>red</sub> (Figure 3) demonstrates that it is the higher stability of the native state and not the mutations per se that causes this change. Thus, stabilization of the native state that suppresses the existence of the aggregation prone molten-globule intermediate at equilibrium also appears to lead to suppression of the transient kinetic molten-globule intermediate and thereby lead to a less off-pathway formation of aggregates.

To demonstrate that the kinetic molten globule exists to a lower extent during refolding of A23C/L203C<sub>ox</sub> than for HCA II<sub>pw<sub>t</sub></sub>, stopped-flow studies of the kinetics of interaction of the molten-globule state with the hydrophobic dye ANS during the refolding process were performed. The presence of the dye from the onset of refolding has been shown to prolong the lifetimes of partially folded states (20). To avoid such complications, we used the ANS-pulsed method described by Engelhard and Evans (21), in which ANS, by sequential mixing, is introduced after folding has been allowed to proceed for a variable time. From the ANS fluorescence intensity developed at various stages of the folding reaction, it can be seen in Figure 4 that the amount

Table 2: Kinetic Parameters of Refolding as Monitored by ANS Binding

protein	$k_1$ (min <sup>-1</sup> ) <sup>a</sup>	$A_1$ <sup>a</sup>	$k_2$ (min <sup>-1</sup> ) <sup>a</sup>	$A_2$ <sup>a</sup>	$r^2$ <sup>b</sup>
HCA II <sub>pw<sub>t</sub></sub>	7.2	0.88	0.04	0.55	0.9950
A23C/L203C <sub>ox</sub>	7.7	0.74	0.23	0.45	0.9984
BCA II	20	0.67	1.1	0.82	0.9907

<sup>a</sup> The rate constants and amplitudes were calculated using a nonlinear fit program (see the Materials and Methods). The amplitudes correspond to the values of the fluorescence signal. <sup>b</sup> The goodness of fit was calculated by the  $r^2$  coefficient of determination.

of molten globule present throughout the reaction (from the shortest detectable aging time; approximately 35 ms) is significantly less for A23C/L203C<sub>ox</sub> than for HCA II<sub>pw<sub>t</sub></sub>. This can be seen very clearly in the inset (Figure 4), reflecting the fast phase during which most of the molten-globule intermediates disappear. This parallel decay with similar rate constants (Table 2) also indicates that the concentration of molten globule is lower for A23C/L203C<sub>ox</sub> than for HCA II<sub>pw<sub>t</sub></sub> during the initial folding stages, before the first observation. Moreover, the slow molten-globule decay phase of A23C/L203C<sub>ox</sub> is almost 6 times faster than that of HCA II<sub>pw<sub>t</sub></sub>, supporting the conclusion that suppression of the molten-globule intermediate during refolding is the main reason for the changed aggregation behavior.

For comparative purposes, the pulsed ANS experiment was repeated for BCA II. Interestingly, the time course for the disappearance of the molten-globule intermediate of BCA II is rather similar to that of A23C/L203C<sub>ox</sub> (Figure 4). The equilibrium unfolding behavior of BCA II is also similar to that of A23C/L203C<sub>ox</sub>, but with a much less pronounced intermediate during GuHCl denaturation than noted for HCA II (22). Thus, the molten-globule state of BCA II, similar to that of A23C/L203C<sub>ox</sub>, is suppressed at equilibrium conditions because of a more stable native state than in HCA II. BCA II incubated in GuHCl at concentrations inducing the molten-globule state, similarly to A23C/L203C<sub>ox</sub>, can be reactivated much more efficiently than is possible for HCA II (23). Reactivation of denatured BCA II at a protein concentration identical to the optimal concentration for refolding of HCA II (0.025 mg/mL) gives a significantly higher reactivation yield for BCA II (90 versus 75%) (19). Although it has been shown that the molten-globule intermediate forms aggregates during refolding, it is quite clear from the comparison above that BCA II is significantly less prone to aggregate than HCA II is. Instead, it behaves very similarly to A23C/L203C<sub>ox</sub> in this respect, most likely because of suppression of the aggregation-prone molten globule also in BCA II.

## CONCLUSIONS

As demonstrated for HCA II, it is possible, by appropriate protein engineering to reconstruct the energy landscape for folding, to circumvent folding traps that, under normal conditions, appear to be impossible to avoid. To conclude, improved refolding yields are possible to achieve, if the emergence of aggregation-prone intermediates, such as the molten globule, can be controlled. A general strategy to circumvent aggregation during refolding of proteins could then be to stabilize the native state of a protein to the extent

that its equilibrium unfolding behavior is converted from a three-state to a two-state process.

## ACKNOWLEDGMENT

We are very grateful to Dr. Per Hammarström and Prof. Bengt-Harald Jonsson, Linköping University, for valuable and critical discussion of the paper.

## REFERENCES

1. Carlsson, U., and Jonsson, B.-H. (1995) Folding of  $\beta$ -sheet proteins, *Curr. Opin. Struct. Biol.* 5, 482–487.
2. Carlsson, U., and Jonsson, B.-H. (2000) Folding and stability of human carbonic anhydrase II, in *The Carbonic Anhydrases New Horizons* (Chegwidden, W. R., Carter, N. D., and Edwards, Y. H., Eds.) pp 241–259, Birkhäuser Verlag, Basel, Switzerland.
3. Eriksson, A. E., Jones, A. T., and Liljas, A. (1988) Refined structure of human carbonic anhydrase II at 2.0-Å resolution, *Proteins: Struct. Funct. Genet.* 4, 274–282.
4. Håkansson, K., Carlsson, M., Svensson, L. A., and Liljas, A. (1992) Structure of native and apo carbonic anhydrase II and structure of some of its anion–ligand complexes, *J. Mol. Biol.* 227, 1192–1204.
5. Mårtensson, L.-G., Jonsson, B.-H., Freskgård, P.-O., Kihlgren, A., Svensson, M., and Carlsson, U. (1993) Characterization of folding intermediates of human carbonic anhydrase II: probing substructure by chemical labeling of SH groups introduced by site-directed mutagenesis, *Biochemistry* 32, 224–231.
6. Svensson, M., Jonasson, P., Freskgård, P.-O., Jonsson, B.-H., Lindgren, M., Mårtensson, L.-G., Gentile, M., Borén, K., and Carlsson, U. (1995) Mapping the folding intermediate of human carbonic anhydrase II. Probing substructure by chemical reactivity and spin and fluorescence labeling of engineered cysteine residues, *Biochemistry* 34, 8606–8620.
7. Hammarström, P., Persson, M., Freskgård, P.-O., Mårtensson, L.-G., Andersson, D., Jonsson, B.-H., and Carlsson, U. (1999) Structural mapping of an aggregation nucleation site in a molten globule intermediate, *J. Biol. Chem.* 274, 32897–32903.
8. Persson, M., Aronsson, G., Bergenhem, N., Freskgård, P.-O., Jonsson, B.-H., Surin, B. P., Spangfort, M. D., and Carlsson, U. (1995) GroEL/ES-mediated refolding of human carbonic anhydrase II: role of N-terminal helices as recognition motifs for GroEL, *Biochim. Biophys. Acta* 1247, 195–200.
9. Mårtensson, L.-G., Karlsson, M., and Carlsson, U. (2002) Dramatic stabilization of the native state of human carbonic anhydrase II by an engineered disulfide bond, *Biochemistry* 41, 15867–15875.
10. Jonasson, P., Aronsson, G., Carlsson, U., and Jonsson, B.-H. (1997) Tertiary structure formation at specific tryptophan side chains in the refolding of human carbonic anhydrase II, *Biochemistry* 36, 5142–5148.
11. Cleland, J. L., and Randolph, T. W. (1992) Mechanism of polyethylene glycol interaction with the molten globule folding intermediate of bovine carbonic anhydrase B, *J. Biol. Chem.* 267, 3147–3153.
12. Persson, M., Carlsson, U., and Bergenhem, N. C. H. (1996) GroEL reversibly binds to, and causes rapid inactivation of, human carbonic anhydrase II at high temperatures, *Biochim. Biophys. Acta* 1298, 191–198.
13. Persson, M., Carlsson, U., and Bergenhem, N. C. H. (1997) GroEL provides a folding pathway with lower apparent activation energy compared to spontaneous refolding of human carbonic anhydrase II, *FEBS Lett.* 411, 43–47.
14. Nozaki, Y. (1972) The preparation of guanidine hydrochloride, *Methods Enzymol.* 26, 43–50.
15. Lindskog, S. (1960) Purification and properties of bovine erythrocyte carbonic anhydrase, *Biochim. Biophys. Acta* 39, 218–226.
16. Khalifah, R. G., Strader, D. J., Bryant, S. H., and Gibson, S. M. (1977) Carbon-13 nuclear magnetic resonance probe of active-site ionizations in human carbonic anhydrase B, *Biochemistry* 16, 2241–2247.
17. Freskgård, P.-O., Carlsson, U., Mårtensson, L.-G., and Jonsson, B.-H. (1991) Folding around the C terminus of human carbonic anhydrase II. Kinetic characterization by use of a chemically reactive SH-group introduced by protein engineering, *FEBS Lett.* 289, 117–122.
18. London, J., Skrzynia, C., and Goldberg, M. E. (1974) Renaturation of *Escherichia coli* tryptophanase after exposure to 8 M urea. Evidence for the existence of nucleation centers, *Eur. J. Biochem.* 47, 409–415.
19. Fransson, C., Freskgård, P.-O., Herbertsson, H., Johansson, Å., Jonasson, P., Mårtensson, L.-G., Svensson, M., Jonsson, B.-H., and Carlsson, U. (1992) Cis–trans isomerization is rate-determining in the reactivation of denatured human carbonic anhydrase II as evidenced by proline isomerase, *FEBS Lett.* 296, 90–94.
20. Itzhaki, L. S., Evans, P. A., Dobson, C. M., and Radford, S. (1994) Tertiary interactions in the folding pathway of hen lysozyme: kinetic studies using fluorescent probes, *Biochemistry* 33, 5212–5220.
21. Engelhard, M., and Evans, P. (1995) Kinetics of interaction of partially folded proteins with a hydrophobic dye: evidence that molten globule character is maximal in early folding intermediates, *Protein Sci.* 4, 1553–1562.
22. Wong, K.-P., and Hamlin, L. (1975) The role of Zn(II) on the folding of bovine carbonic anhydrase B, *Arch. Biochem. Biophys.* 170, 12–22.
23. Andersson, D., Hammarström, P., and Carlsson, U. (2001) Cofactor-induced refolding: refolding of molten globule carbonic anhydrase induced by Zn(II) and Co(II), *Biochemistry* 40, 2653–2661.

BI049709Z